

Molecular modeling of potential PET imaging agents for adenosine receptor in Parkinson's disease

Z. Tamiji¹ · M. Salahinejad²  · A. Niazi¹

Received: 19 August 2017 / Accepted: 3 October 2017 / Published online: 28 October 2017
© Springer Science+Business Media, LLC 2017

Abstract The adenosine receptors have appeared as potent and selective drug target in various diseases especially for central nervous system diseases. Adenosine receptor A_{2A} antagonists have been known as potential treatment for Parkinson's disease (PD). Radiolabeled A_{2A}R antagonists can be used as positron emission tomography (PET) tracers and diagnostic tools for PD. In the present investigation, we perform the quantitative structure–activity relationship (QSAR) analysis and docking studies of a series of PET tracers as ligands and Adenosine receptors (A_{2A}R) binding affinity, to elucidate the structural properties required for A_{2A}R antagonist in treatment for PD. Several variable-selection methods were used to choose the descriptors that would lead to good QSAR model. Among several models developed, the best model was a five-variable multiple linear regression (MLR) equation with statistical parameters of squared correlation coefficient $R^2 = 0.90 \pm 0.01$ and cross-validated correlation coefficient $Q^2 = 0.84 \pm 0.02$. The QSAR models were also constructed for A_{2A}R selectivity to tracer ligands, that yielded a four-variable model with $R^2 = 0.94 \pm 0.01$ and $Q^2 = 0.89 \pm 0.02$. The most important variables contributed in models construction involved: partial charge, hydrophobic atoms, rotatable bonds, polar van der

Waals surface area, potential energy, and conformation-dependent charge descriptors. Finally, molecular docking analysis was carried out to better understand the interactions between ligands and Adenosine receptors. The importance of π - π stacking interactions between aromatic moiety of the ligands and triazine core of A_{2A}R antagonist was confirmed.

Keywords Adenosine receptors · Positron emission tomography (PET) · Quantitative structure–activity relationship (QSAR) · Docking

Introduction

In recent years, the adenosine receptors have appeared as potential drug targets [1, 2]. Adenosine, a purine nucleoside, is an endogenous modulator of a number of physiological functions in the central nervous system (CNS) as well as in peripheral tissues [3–5]. These receptors have been extensively characterized and divided into four different subtypes including: A₁, A_{2A}, A_{2B}, and A₃ [4]. It acts at specific membrane G-protein receptors positively (A_{2A}, A_{2B}) or negatively (A₁, A₃) linked to adenylatecyclase [4]. Among these four subtype adenosine receptors in the CNS, the adenosine A_{2A} receptors (AR) are densely distributed in the central nervous system (striatum, nucleus accumbens, and olfactory tubercles) which controls intracellular AMP (Adenosine monophosphate) levels and play an important role in the regulation of mood and motor function [6]. Adenosine A_{2A} receptor antagonists have developed as potential treatment for Parkinson's disease in the past decade [7, 8].

Human Parkinson's disease (PD) is a very serious neurological disorder, and current manner of treatment fail to achieve long-term control. Since adenosine receptors antagonists have been shown to restore the deficits arise from decline

✉ M. Salahinejad
salahinejad@gmail.com

Z. Tamiji
zahra.tamiji@gmail.com

A. Niazi
ali.niazi@gmail.com

¹ Department of Chemistry, Faculty of Science, Arak Branch, Islamic Azad University, Arak, Iran

² Nuclear Science and Technology Research Institute, Tehran, Iran

of the striatonigral dopamine system, which is compromised by the loss of striatal neurons in this disease, A_{2A} antagonism provides a possible treatment for PD [9]. Dopamine receptors, as a subclass of G protein-coupled receptors, are important in the vertebrate central nervous system. The existence of multiple types of receptors for dopamine was first proposed in 1976 [10]. There are at least five subtypes of dopamine receptors, D_1 , D_2 , D_3 , D_4 , and D_5 . Excitation of the A_{2A} receptor was found to reduce the binding desire of dopamine D_2 receptors for dopamine and to counter the actions of both D_1 and D_2 receptors on behavior, gene expression, and secondary messenger systems [11, 12]. Consequently, blockade of the adenosine receptor could compensate for the lack of dopamine D_2 receptor-mediated control of striato-Gpe neurons [12]. At the moment, a number of pharmacological models that can recapitulate many of the symptoms displayed in Parkinsonian patients such as bradykinesia, rigidity, and tremor, and A_{2A} receptor antagonists appeared to have a useful effect in many of these models [13–18].

Positron emission tomography (PET) [19, 20] is the most advanced methods for non-invasive medical imaging modality that provides 3D maps of the brain. PET studies show better accuracy and resolution in quantification of regional distribution and temporal measurements of radioactivity and thus are superior to all other imaging modalities including single photon emission computed tomography (SPECT) [21, 22]. Both agonist and antagonist ligands containing positron emitting radioisotopes have been introduced for 3-dimensional in vivo imaging of the receptors [23]. Such ligands for PET might prove useful for eventual diagnostic use in the CNS. Ligands for in vivo PET imaging of A_1 , A_{2A} , and A_{3A} Rs have been developed. A_{2A} R antagonist PET tracers are of two types, xanthine and non-xanthine PET tracers [24, 25]. Development of new ligands that may lead to new candidates for PET tracer to improve physicochemical and pharmacokinetics properties and mapping adenosine receptors is of great interest.

The search for new compounds with desired properties requires enormous human resource and cost. That is why the pharmaceutical industry has shown great interest in theoretical approaches that enable the logical design of pharmaceutical agents. Quantitative structure-activity relationships (QSAR) studies, as significant research fields in drug design and medicinal chemistry, have obtained an important place within modern chemistry and therefore, there exists a keen interest on the development of these techniques [26–28]. The purpose of QSAR approaches is to develop some quantitative models to predict activity of a compound, and these models can reduce the research time and cost of new drugs.

In this study, we built the QSAR model with molecular descriptors, to explore the correlations of the molecular structure of a series of PET tracers as ligands and for A_{2A} receptor antagonist binding affinity and selectivity of the tracer between A_1 and A_{2A} receptors. Molecular docking analysis

was also carried out to better understand the interactions between ligands and Adenosine receptors.

Methods

Data set The data set employed for the QSAR analyses contains 35 Xanthine ligands as A_{2A} R antagonist PET tracers were taken from the literature [29] and applied for QSAR analysis. The structures of all the compounds along with their experimental binding affinity and selectivity are presented in Table 1. The A_{2A} R selectivity ($S_{A_{2R}}$) and binding affinity ($A_{A_{2R}}$) values ranged between 0.1–20 and 7.84–16,500 nM, respectively. These values were converted into the corresponding logarithm values and utilized as dependent variables.

Descriptor calculation Optimized and energy-minimized structures of the molecules were used to calculate molecular descriptors. The energy minimization of the molecules was done using AM₁ (Austin model) Hamiltonian method available in MOPAC module with a convergence criterion of 0.001 kcal/molÅ. Various kinds of molecular descriptors involving: physicochemical, structural, partial charge, topological, and geometrical descriptors were computed using Molecular Operating Environment (MOE, Chemical Computing Group Inc. 2011) package.

As a first step in variables reduction, descriptors exhibiting constant or nearly constant values as well as those with poor correlation to the dependent variables ($R^2 < 0.10$) were removed.

Descriptor selection Feature selection is of considerable importance in QSAR modeling to reduce the computational complexity, improving the prediction performance of constructed models and providing a better understanding of the underlying process [30]. Three feature selection procedures including: genetic algorithm (GA), enhanced replacement method (ERM), genetic function approximation (GFA), and stepwise multiple linear regression (stepwise-MLR) were applied to choose the best subset of descriptors out of a large pool of descriptors.

Genetic algorithms Genetic algorithms (GA), explained by Holland [31], mimic natural evolution and selection. In biological systems, genetic data that distinguishes the individuality of an organism is stored in chromosomes. Chromosomes are replicated and passed onto the next generation with selection criteria depending on fitness. Genetic information can however be changed through genetic operations such as crossover and mutation.

Table 1 Structures and experimental A_{2A}R selectivity and A_{2A}R binding affinity for A_{2A}R antagonist PET tracers

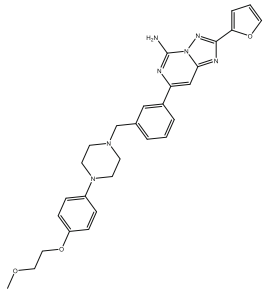
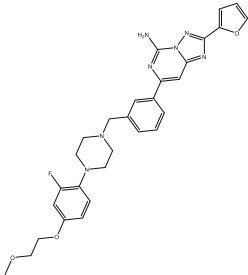
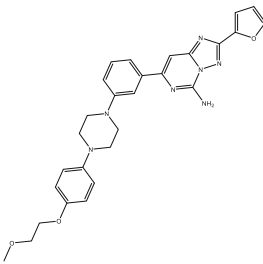
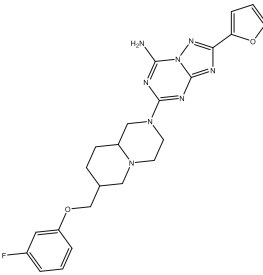
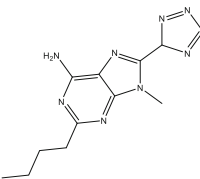
Structures and experimental A _{2A} R-selectivity and A _{2A} R Binding affinity for A _{2A} R antagonist PET tracers				
Compd. no.	Structure	Name	A _{2A} (nm)	Selectivity
1		2-(furan-2-yl)-7-(3-((4-(2-methoxyethoxy)phenyl)piperazin-1-yl)methyl)phenyl)-[1,2,4]triazolo[1,5-f]pyrimidin-5-amine	2.8	601
2		7-(3-((4-(2-fluoro-4-(2-methoxyethoxy)phenyl)piperazin-1-yl)methyl)phenyl)-2-(furan-2-yl)-[1,2,4]triazolo[1,5-f]pyrimidin-5-amine	2.7	642
3		2-(furan-2-yl)-7-(3-(4-(4-(2-methoxyethoxy)phenyl)piperazin-1-yl)phenyl)-[1,2,4]triazolo[1,5-f]pyrimidin-5-amine	1	1059
4		5-(7-((3-fluorophenoxy)methyl)-hexahydro-1H-pyrido[1,2-a]pyrazin-2(6H)-yl)-2-(furan-2-yl)-[1,2,4]triazolo[1,5-a][1,3,5]triazin-7-amine	0.2	16500
5		2-butyl-9-methyl-8-(3H-1,2,4-triazol-3-yl)-9H-purin-6-amine	6.6	11.92

Table 1 (continued)

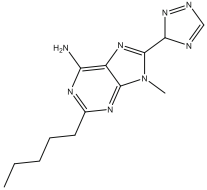
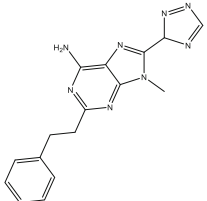
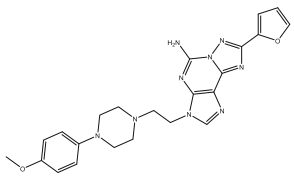
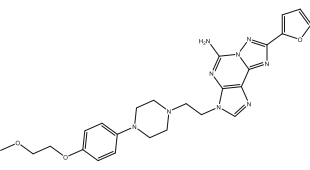
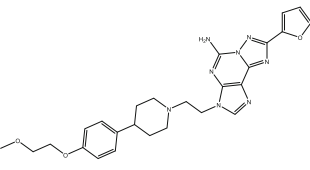
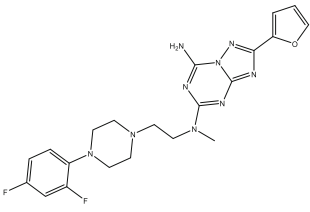
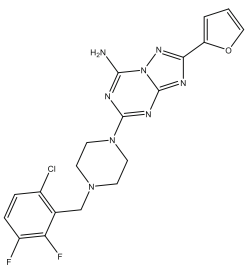
6		9-methyl-2-pentyl-8-(3H-1,2,4-triazol-3-yl)-9H-purin-6-amine	3.3	7.84
7		9-methyl-2-phenethyl-8-(3H-1,2,4-triazol-3-yl)-9H-purin-6-amine	4.7	17.02
8		8-(furan-2-yl)-3-(2-(4-(4-methoxyphenyl)piperazin-1-yl)ethyl)-3H-[1,2,4]triazolo[1,5-g]purin-5-amine	0.1	1695
9		8-(furan-2-yl)-3-(2-(4-(4-(2-methoxyethoxy)phenyl)piperazin-1-yl)ethyl)-3H-[1,2,4]triazolo[1,5-g]purin-5-amine	0.9	669
10		8-(furan-2-yl)-3-(2-(4-(4-(2-methoxyethoxy)phenyl)piperidin-1-yl)ethyl)-3H-[1,2,4]triazolo[1,5-g]purin-5-amine	0.7	519
11		N5-(2-(4-(2,4-difluorophenyl)piperazin-1-yl)ethyl)-2-(furan-2-yl)-N5-methyl-[1,2,4]triazolo[1,5-a][1,3,5]triazine-5,7-diamine	4	205
12		5-(4-(6-chloro-2,3-difluorobenzyl)piperazin-1-yl)-2-(furan-2-yl)-[1,2,4]triazolo[1,5-a][1,3,5]triazin-7-amine	5	100

Table 1 (continued)

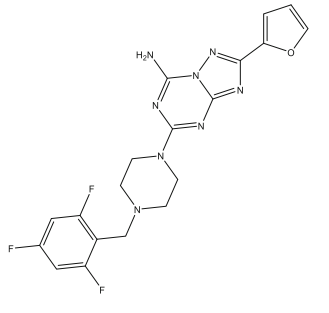
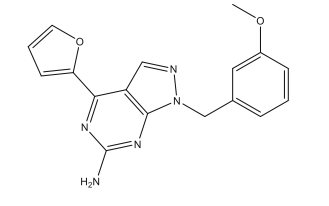
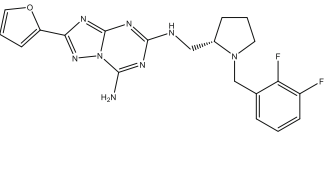
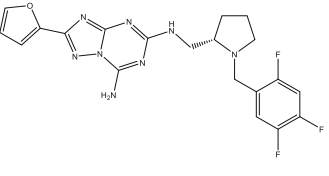
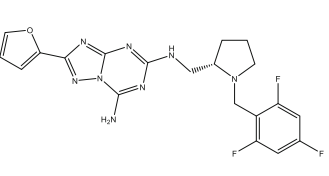
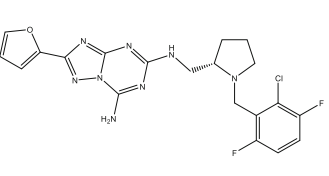
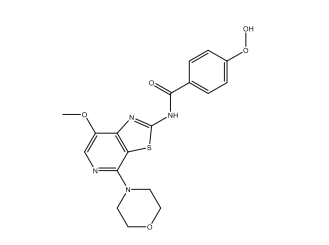
13		2-(furan-2-yl)-5-(4-(2,4,6-trifluorobenzyl)piperazin-1-yl)-[1,2,4]triazolo[1,5-a][1,3,5]triazin-7-amine	3	433
14		4-(furan-2-yl)-1-(3-methoxybenzyl)-1H-pyrazolo[3,4-d]pyrimidin-6-amine	2	-
15		(S)-N5-((1-(2,3-difluorobenzyl)pyrrolidin-2-yl)methyl)-2-(furan-2-yl)-[1,2,4]triazolo[1,5-a][1,3,5]triazine-5,7-diamine	5	250
16		(S)-2-(furan-2-yl)-N5-((1-(2,4,5-trifluorobenzyl)pyrrolidin-2-yl)methyl)-[1,2,4]triazolo[1,5-a][1,3,5]triazine-5,7-diamine	8	250
17		(S)-2-(furan-2-yl)-N5-((1-(2,4,6-trifluorobenzyl)pyrrolidin-2-yl)methyl)-[1,2,4]triazolo[1,5-a][1,3,5]triazine-5,7-diamine	2	800
18		(S)-N5-((1-(2-chloro-3,6-difluorobenzyl)pyrrolidin-2-yl)methyl)-2-(furan-2-yl)-[1,2,4]triazolo[1,5-a][1,3,5]triazine-5,7-diamine	4	250
19		4-hydroperoxy-N-(7-methoxy-4-morpholinothiazolo[5,4-c]pyridin-2-yl)benzamide	3	450

Table 1 (continued)

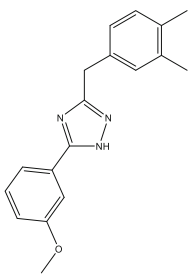
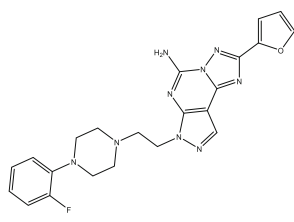
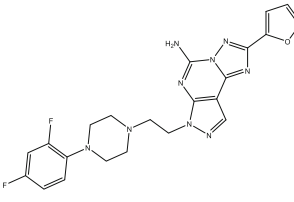
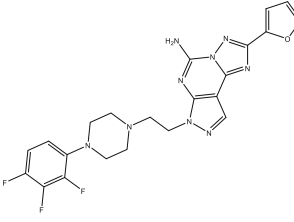
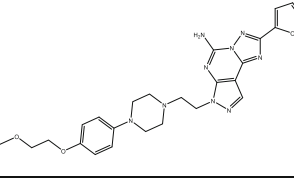
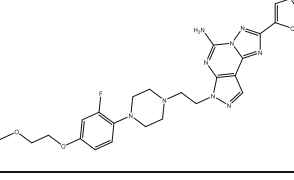
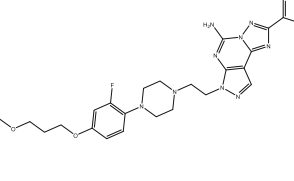
20		3-(3,4-dimethylbenzyl)-5-(3-methoxyphenyl)-1H-1,2,4-triazole	20	69
21		7-(2-(4-(2-fluorophenyl)piperazin-1-yl)ethyl)-2-(furan-2-yl)-7H-pyrazolo[4,3-e][1,2,4]triazolo[1,5-c]pyrimidin-5-amine	0.6	894
22		7-(2-(4-(2,4-difluorophenyl)piperazin-1-yl)ethyl)-2-(furan-2-yl)-7H-pyrazolo[4,3-e][1,2,4]triazolo[1,5-c]pyrimidin-5-amine	0.6	1600
23		2-(furan-2-yl)-7-(2-(4-(2,3,4-trifluorophenyl)piperazin-1-yl)ethyl)-7H-pyrazolo[4,3-e][1,2,4]triazolo[1,5-c]pyrimidin-5-amine	0.6	1498
24		2-(furan-2-yl)-7-(2-(4-(4-(2-methoxyethoxy)phenyl)piperazin-1-yl)ethyl)-7H-pyrazolo[4,3-e][1,2,4]triazolo[1,5-c]pyrimidin-5-amine	1.1	1340
25		7-(2-(4-(2-fluoro-4-(2-methoxyethoxy)phenyl)piperazin-1-yl)ethyl)-2-(furan-2-yl)-7H-pyrazolo[4,3-e][1,2,4]triazolo[1,5-c]pyrimidin-5-amine	0.4	1736
26		7-(2-(4-(2-fluoro-4-(3-methoxypropoxy)phenyl)piperazin-1-yl)ethyl)-2-(furan-2-yl)-7H-pyrazolo[4,3-e][1,2,4]triazolo[1,5-c]pyrimidin-5-amine	0.6	1158

Table 1 (continued)

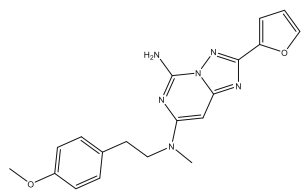
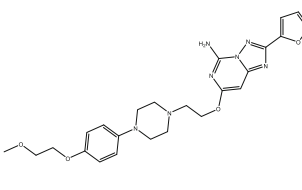
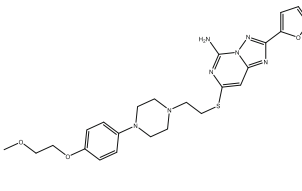
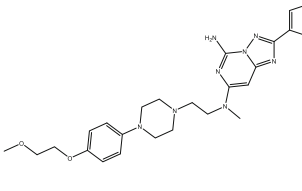
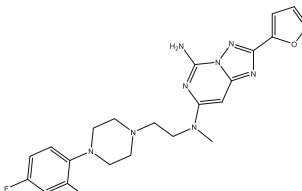
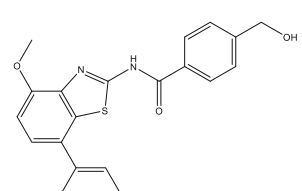
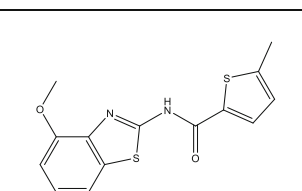
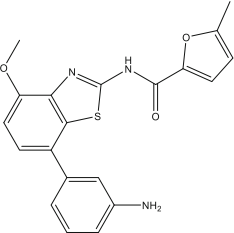
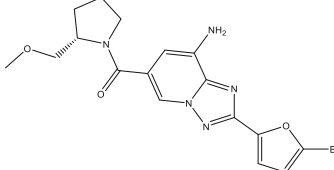
27		2-(furan-2-yl)-N7-(4-methoxyphenethyl)-N7-methyl-[1,2,4]triazolo[1,5-f]pyrimidine-5,7-diamine	1.8	473
28		2-(furan-2-yl)-7-(2-(4-(4-(2-methoxyethoxy)phenyl)piperazin-1-yl)ethoxy)-[1,2,4]triazolo[1,5-f]pyrimidin-5-amine	2.8	405
29		2-(furan-2-yl)-7-(2-(4-(4-(2-methoxyethoxy)phenyl)piperazin-1-yl)ethylthio)-[1,2,4]triazolo[1,5-f]pyrimidin-5-amine	1.5	965
30		2-(furan-2-yl)-N7-(2-(4-(4-(2-methoxyethoxy)phenyl)piperazin-1-yl)ethyl)-N7-methyl-[1,2,4]triazolo[1,5-f]pyrimidine-5,7-diamine	1	1580
31		N7-(2-(4-(2,4-difluorophenyl)piperazin-1-yl)ethyl)-2-(furan-2-yl)-N7-methyl-[1,2,4]triazolo[1,5-f]pyrimidine-5,7-diamine	2.5	694
32		4-(hydroxymethyl)-N-(4-methoxy-7-phenylbenzo[d]thiazol-2-yl)benzamide	0.5	-
33		N-(7-(3-aminophenyl)-4-methoxybenzo[d]thiazol-2-yl)-5-methylthiophene-2-carboxamide	0.8	-

Table 1 (continued)

34		N-(7-(3-aminophenyl)-4-methoxybenzo[d]thiazol-2-yl)-5-methylfuran-2-carboxamide	1	-
35		(S)-(8-amino-2-(5-bromofuran-2-yl)-[1,2,4]triazolo[1,5-a]pyridin-6-yl)(2-(methoxymethyl)pyrrolidin-1-yl)methanone	16	65.8

Genetic function approximation (GFA) GFA is a helpful technique for searching in a large parameter space when the data is small. This technique can choose descriptors automatically and optimize parameters, expand a population of models simultaneously, and avoid local optima. Models are improved by performing a crossover operation to recombine terms of better scoring models. GFA technique is a method using the idea of natural selection and evolution in higher dimensional space to choose optimal descriptor combinations able of explaining bioactivity variation among training compounds from a large pool of possible descriptor combinations [32, 33].

The best subset selection version 1.2 program available at https://teqip.jdvu.ac.in/QSAR_Tools/ was used to carry out the GFA variable selection.

Enhanced replacement method Enhanced replacement method (ERM) suggested by Mercader et al. [34] is an improved version of replacement method (RM) [35, 36]. This technique approaches the minimum of S by judiciously taking into account the relative errors of the coefficients of the least-squares model given by a set of d descriptors $d = X_1, X_2, \dots, X_d$.

$$SD^2 = \frac{1}{N-d-1} \sum_{i=1}^N res_i^2 \quad (1)$$

In this equation, N is the number of molecules in the set of train, and res_i the residual for molecule i , the difference between the experimental activity and predicted activity. More detailed information about these algorithms can be found in reference [34].

Stepwise-multiple linear regressions Stepwise-MLR, a multiple-term linear equation was constructed step-by-step. The basic approach contains (1) recognized an initial model,

(2) iteratively “stepping,” that is, frequently altering the model at the previous step by adding or removing a predictor variable in accordance with the “stepping criteria,” and (3) terminating the research when stepping is no longer possible given the stepping criteria, or when a specified maximum number of steps have been attained. Especially, at each step all variables are reviewed and evaluated to determine which one will contribute most to the equation. That variable is then contained in the model, and the process starts again.

Model construction and validation The data set was randomly divided into a training set (80%), which was used to adjust the parameters of the models, and a test set (20%) to evaluate the prediction ability of the models obtained.

QSAR models were generated for this series using multiple linear regression (MLR) and partial least squares (PLS) regression methods and those which come out with promising results are discussed here.

For each model cross-validated correlation coefficient (Q^2), correlation coefficients of calibration of train set (R^2_{train}), correlation coefficient of prediction set (R^2_{pred}), root mean square error of calibration (RMSEC) and root mean square error of prediction (RMSEP) were calculated. Y -randomization test was also applied to internally validate the models obtained. In Y -randomization test, the model was reconstructed based on randomized values of Y variable. The correlation coefficients of randomization ($R^2_{Y\text{rand}}$) values imply that acceptable models were obtained for the given data sets by the current modeling method and they did not show any chance correlation [37]. The external validation of final model was also checked by mean absolute error (MAE) based criteria [38]. The applicability domain (AD) of final QSAR models was explored based on standardization approach proposed by Roy et al. [39].

Table 2 Statistical parameters of models by QSAR for prediction power A_{2A}R Binding affinity.

Model	RMSEc	RMSEp	RMSEcv	R ² _{train}	Q ²	R ² _{pred}	R ² _{Yrand}	No. of vars
Stepwise MLR	0.18±0.02	0.22±0.06	0.24±0.03	0.87±0.02	0.78±0.06	0.79±0.08	0.18±0.03	5
GFA – MLR	0.22±0.02	0.26±0.09	0.29±0.04	0.80±0.04	0.68±0.08	0.71±0.22	0.17±0.02	4
GA - PLS	0.27±0.02	0.27±0.11	0.37±0.04	0.72±0.05	0.56±0.07	0.72±0.12	0.18±0.02	6
ERM – MLR	0.16±0.01	0.19±0.04	0.20±0.01	0.90±0.01	0.84±0.02	0.80±0.15	0.17±0.01	5

The significance level of 0.05 was set for all calculations

Molecular docking

For the present docking study, AutoDock program, version 4.1.1, was adopted. Discovery Studio Visualizer (Accelrys Software Inc) and Pymol (The PyMOL Molecular Graphics System) programs were employed for docking simulation. Fine 3D structure with a resolution of 3.27 Å of Adenosine A_{2A} receptor was retrieved from the Protein Data Bank (PDB ID, 3UZA).

All of the compounds in the dataset were docked into the binding site of Adenosine receptor to provide the interaction between the ligand and the receptor. Initially, for the purpose of docking studies, the protein was considered without ligand and water molecules. Hydrogen atoms and the active torsions of ligand were assigned using Autodock Tools (ADT). AutoGrid was employed to generate grid maps around the active site. The volume of the grid was set to cover the binding site with a grid-spacing interval of 1.0 Å with dimensions of 40 × 40 × 40 Å. When docking was performed, some residues in the protein active site and all the torsional bonds in the ligand were set free. Lamarckian Genetic Algorithm (LGA) was employed then for conformational search with standard protocol. The final structures were clustered and ranked according to the Autodock scoring function.

Results and discussion

Tables 2 and 3 represent the statistical performance of model obtained based on selected descriptors with different variable selection methods for A_{2A}R binding affinity and selectivity respectively. GFA, ERM, GA, and stepwise procedures were used for variable selection. MLR and PLS methods were used to build models. The number of descriptors base on the

statistical parameters arriving from the models with different number of descriptors. From Tables 2 and 3, it is observed that for all the models the data fit ($R^2 = 0.68–0.92$) and the predictive capability of models ($R^2_{pred} \geq 0.68$) is acceptable.

The best QSAR model obtained for A_{2A}R binding affinity was ERM-MLR, although the stepwise-MLR model showed similar statistical performance (Table 2). The multiple linear regressions based on ERM-selected descriptors, were performed to set up a statistically reliable model with good predictive ability for A_{2A}R binding affinity including: $R^2_{train} = 0.90 \pm 0.01$, $Q^2 = 0.84 \pm 0.02$, and $R^2_{pred} = 0.80 \pm 0.15$. The optimal QSAR model of A_{2A}R binding affinity according to ERM-MLR was

$$\begin{aligned} \text{Log}(A_{A2R}) = & -(8.77 \pm 0.01) + (0.33 \pm 0.01) \text{ density} \quad (2) \\ & -(0.24 \pm 0.01) \text{ Q_VSA_POL} \\ & -(1.3 \pm 0.10) \text{weinerPol} + (1.46 \pm 0.11) \text{Kier1} \\ & -(0.40 \pm 0.01) \text{E_ang.} \end{aligned}$$

Both of density and Kier1 descriptors, which represent the molecular shapes, showed positive effect impact on binding affinity whereas weinerPol descriptor as a distance-based molecular structure showed negative impact on binding affinity. Q_VSA_POL describes the total polar van der Waals surface area of molecules and showed negative impact on binding affinity. Table 4 gives a brief description of the most important descriptors which selected and involved in all constructed QSAR models for binding affinity. The capacity factor descriptors (vsurf_CW1 and vsurf_CW2) represent hydrophilic regions and computed as the ratio of hydrophilic surface on the overall molecule surface. GCUT_SLOGP descriptors represent the atomic contribution to logP (octanol-water partition coefficient). Most of involved descriptors indicate on the importance of partial charge properties and volume, shape, and subdivided surface

Table 3 Statistical parameters of models by QSAR for prediction power A_{2A}R-selectivity

Model	RMSEc	RMSEp	RMSEcv	R ² _{train}	Q ²	R ² _{pred}	R ² _{Yrand}	No. of vars
Stepwise MLR	0.20±0.01	0.24±0.03	0.30±0.05	0.92±0.01	0.84±0.04	0.81±0.01	0.24±0.03	5
GFA – MLR	0.20±0.01	0.23±0.03	0.29±0.03	0.92±0.01	0.84±0.02	0.78±0.18	0.21±0.03	4
GA - PLS	0.21±0.01	0.45±0.10	0.62±0.23	0.91±0.01	0.52±0.16	0.72±0.05	0.48±0.07	6
ERM – MLR	0.17±0.01	0.18±0.06	0.23±0.03	0.94±0.01	0.89±0.02	0.88±0.01	0.21±0.02	4

The significance level of 0.05 was set for all calculations

Table 4 Selected descriptors for the QSAR study of A_{2A}R binding affinity

Density	Molecular mass density: weight divided by vdw_vol.
Dipole y	The y component of the dipole moment (external coordinates).
E_ang	Angle bend potential energy. In the Potential Setup panel, the term enable flag is ignored, but the term weight is applied.
GCUT_SLOGP_3	The GCUT descriptors using atomic contribution to log P (using the Wildman and Crippen SlogP method) instead of partial charge.
Kier1	First kappa shape index: $(n-1)^2/m^2$
Q_VSA_POL	Total polar van der Waals surface area. This is the sum of the v_i such that $ q_i $ is greater than 0.2. The v_i are calculated using a connection table approximation.
vsurf_CW1	Capacity factor
vsurf_CW2	Capacity factor
WeinerPol	Wiener polarity number: half the sum of all the distance matrix entries with a value of 3 as defined in [Balaban 1979].

area properties of Xanthine ligands, as PET tracer, on binding affinity to A_{2A}R.

Table 3 showed the statistical performance of different QSAR models obtained based on selected descriptor of various variable selections for A_{2A}R selectivity to Xanthine ligands. As could be seen, the best QSAR model obtained for A_{2A}R selectivity was ERM-MLR with five variables. The multiple linear regressions based on ERM-selected descriptors, were performed to set up a statistically reliable model with good predictive ability for A_{2A}R selectivity including $R^2_{\text{train}} = 0.94 \pm 0.01$, $Q^2 = 0.89 \pm 0.02$, and $R^2_{\text{pred}} = 0.88 \pm 0.01$. The optimal QSAR model of A_{2A}R selectivity according to ERM-MLR was

$$\begin{aligned} \text{Log}(S_{A2R}) = & (2.62 \pm 0.03) + (0.65 \pm 0.02)PEOE_PC^- \\ & -(0.41 \pm 0.01)b_rotR + (0.65 \pm 0.01)E_ang \\ & -(0.79 \pm 0.02)PC^- \end{aligned} \quad (3)$$

Total negative partial charge (PEOE_PC-) and angle bend potential energy (E_ang) with positive regression coefficients

showed positive impact on selectivity of A_{2A}R. The next two variables, namely b_rotR, that calculate fraction of rotatable bonds, and PC-, which describes the negative partial charge, have negative contributions to the A_{2A}R selectivity to Xanthine ligands.

Table 5 represents a brief description of the most important descriptors which selected and involved in all constructed models for A_{2A}R selectivity to Xanthine ligands. The vsurf_DW23 descriptor intends to describe lipophilicity and vsurf_IW1 represent hydrophilic regions of a molecule. As could be obvious from Table 5, the molecular flexibility and electrostatic interactions play important role in the selectivity of adenosine A_{2A} receptor to Xanthine ligands.

Xanthine ligands that show high affinity and selectivity to A_{2A}R antagonists usually contain alkyl/alkynyl moieties at N atoms of Xanthine backbone [40]. The ability of Xanthine ligand to form hydrogen bonding and steric hindrances in molecular structure has considerable impact on A_{2A}R selectivity and A_{2A}R binding affinity.

Table 5 Selected descriptors for the QSAR study of A_{2A}R selectivity

Descriptor	Description
a_hyd	Number of hydrophobic atoms
b_rotN	Number of rotatable bonds. A bond is rotatable if it is not in a ring, and neither atom of the bond is such that $(d_i + h_i) < 2$.
BCUT_SLOGP_0	The BCUT descriptors using atomic contribution to logP (using the Wildman and Crippen SlogP method) instead of partial charge.
BCUT_SMR_2	The BCUT descriptors using atomic contribution to molar refractivity (using the Wildman and Crippen SMR method) instead of partial charge.
E_ang	Angle bend potential energy. In the Potential Setup panel, the term enable flag is ignored, but the term weight is applied.
GCUT_SMR_3	The GCUT descriptors using atomic contribution to molar refractivity (using the Wildman and Crippen SMR method) instead of partial charge.
PC+	Total positive partial charge.
PEOE_VSA + 0	Sum of v_i where q_i is in the range (0.00, 0.05).
rings	The number of rings.
vsurf_DW23	Contact distances of vsurf_EWmin.
vsurf_IW1	Hydrophilic integrity moment.

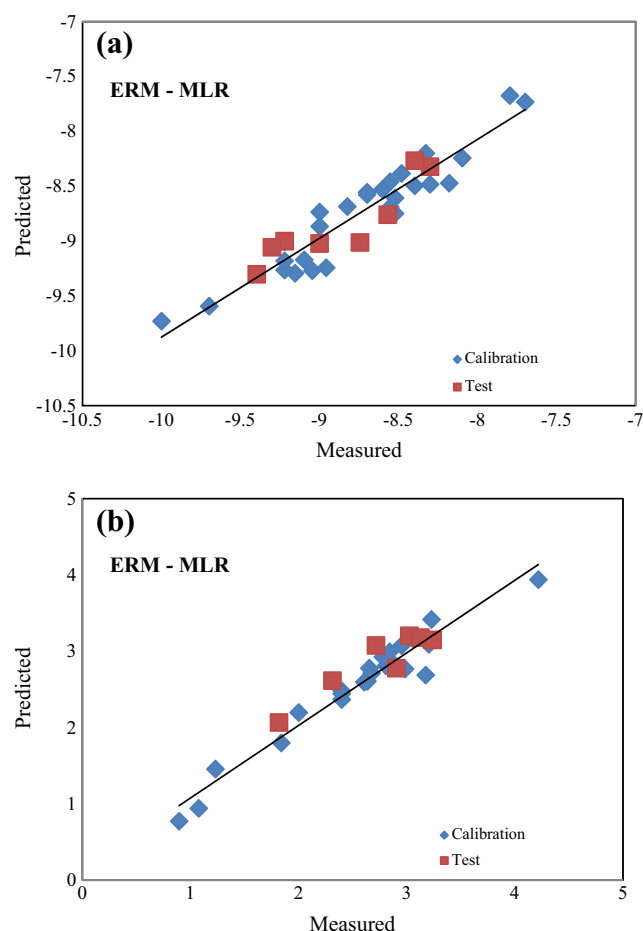


Fig. 1 The fitted values resulting from linear models on the x -axis relative to the experimental values on the y -axis for ERM-MLR method for (a) binding affinity and (b) selectivity of PET tracer ligands to A_{2A} antagonist

Figure 1 compares the experimental and the predicted values of A_{2A} R selectivity and A_{2A} R binding affinity for ERM-MLR models.

Table 6 shows the performance parameters of MAE-based criteria for validation tests of A_{2A} R binding affinity and selectivity QSAR models. MAE and $MAE + 3\delta$ values, concordance correlation coefficient (CCC), Q^2_{F1} , and Q^2_{F2} [41] were calculated for both QSAR models. These parameters were calculated using “Xternal Validation Plus” tool that is freely available at <http://dtclab.webs.com/software-tools>. As can be seen from Table 6, both QSAR models show high values for CCC, Q^2_{F1} , and Q^2_{F2} indicating the reliability and high-performance prediction of proposed models to estimate and predict new compounds A_{2A} R selectivity and A_{2A} R binding

affinity. If a QSAR model follows the criteria: $MAE \leq 0.1 \times$ data range and $MAE \pm 3\sigma \leq 0.2 \times$ data range, then the model could be considered as good predictor. From Table 6, these criteria are preset in both final QSAR models.

The performance of models obtained from prediction errors was shown in Table 6. The values of variance, $Bias^2$ and mean square error (MSE) parameters confirm no systematic error in quantitative predictions.

The applicability domain (AD), as a tool to check the reliability of prediction power of QSAR models, was calculated using “Applicability domain using standardization approach” freely available at <http://dtclab.webs.com/software-tools>. The AD analysis of the A_{2A} R binding affinity model reveals that one outlier in train set (compound 2, Table 1). Removing of compound considered as outlier had no significant effect on the predictive power of the model. The AD analysis of the A_{2A} R selectivity model show no outliers in both train and test set.

Molecular docking

Molecular docking studies of these compounds with adenosine A_{2A} receptor represented very good binding interactions and warrants further studies to corroborate their binding with human A_{2A} receptor for the design and development of better treatment for PD. All of the ligands were docked into the active site of A_{2A} receptor to study the possible mode of their interactions. Docking of these ligands into inhibitor binding cavity of A_{2A} R confirms that these ligands dock in a similar binding modus like native co-crystallized ligand (Fig. 2). Inhibitor binding cavity of A_{2A} R is predetermined by residues Ile-66, Ala-63, Leu-85, Phe-168, Met-177, Leu-249, His-250, Asn-253, Ala-277, Ile-274, T4g-330, and His-278. Analysis of the receptor/ligand complex models generated after successful docking of the compounds was based on parameters such as (1) hydrogen bond interactions, (2) hydrophobic interaction, (3) binding energy, (4) RMSD of active site residues and (5) orientation of the docked compound within the active site (Fig. 3). Lowest RMSD value was 1.37 Å (for compound 14) and RMSD value lower or close to 2 Å was considered as a successful docking [42]. In this research, RMSD values were within 2.0 Å representing our docking methods are valid for the given structures.

The most powerful ligand was selected to perform the docking study in the dataset. Figure 3 shows the several of

Table 6 Performance parameters from validation of QSAR models obtained

Model	Data range	MAE	MAE + 3 δ	Range \times 0.1	Range \times 0.2	CCC	Q^2_{F1}	Q^2_{F2}	Variance	$Bias^2$	MSE
Log($A_{2A}R$)	7.82	0.137	0.356	0.782	0.1564	0.940	0.999	0.889	0.0407	0.1395	0.0895
Log(S_{A2R})	7.82	0.123	0.367	0.782	0.1564	0.965	0.998	0.932	0.0512	0.1486	0.01121

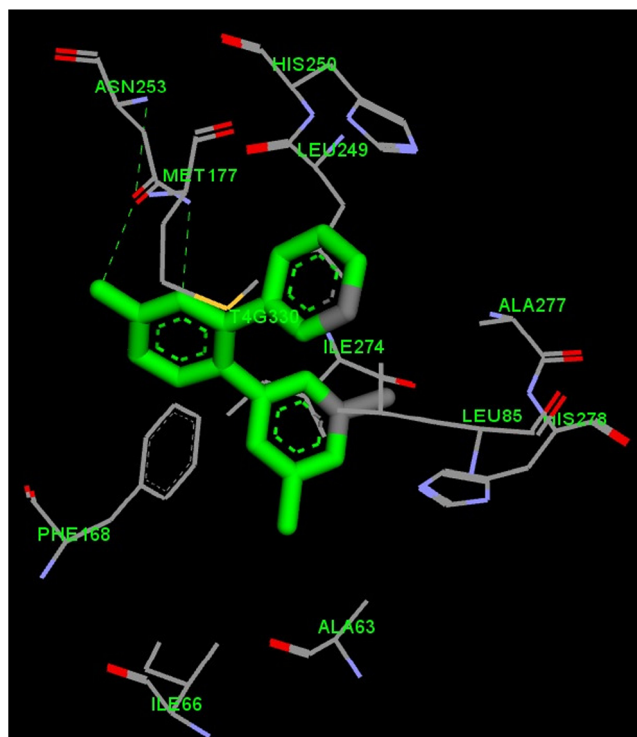


Fig. 2 The docking of the native co-crystallized ligand with protein binding site

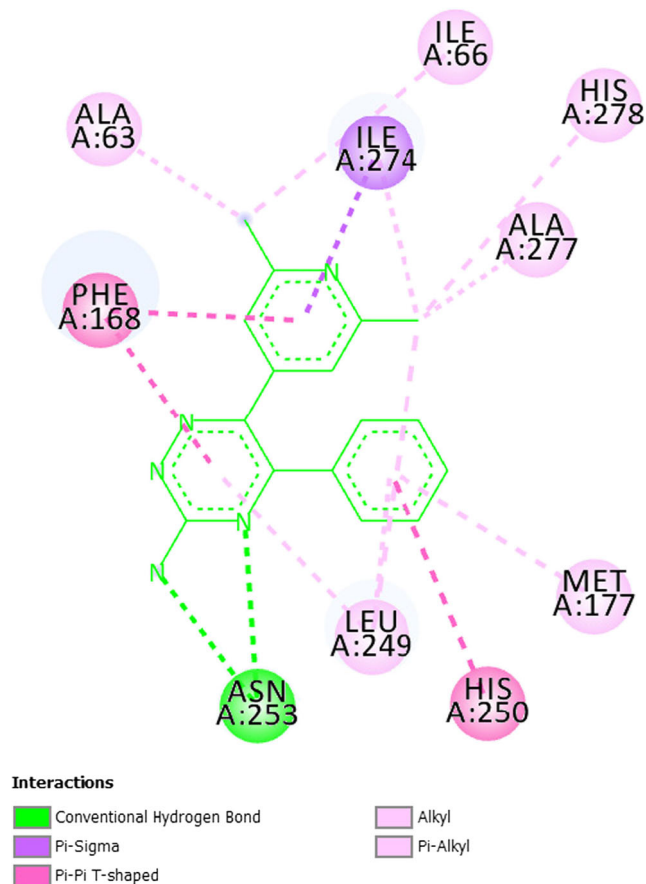


Fig. 3 The ligand interactions profile

interactions between the ligand and the receptor. An aromatic π - π stacking between aromatic ligand with Phe168 for all ligands was the common interaction pattern. An amino group of the ligand as hydrogen bond donor has main role in the high-affinity ligands and with side chain of the conserved Asn253 are established the powerful polar interactions. Also, a hydrophobic interaction between amino triazine core and the side chain of Asn253 can be observed.

Conclusions

As a first study on QSAR modeling of binding affinity and selectivity of Xanthine PET tracers to $A_{2A}R$ antagonist, different modeling strategies including ERM-MLR, GA-PLS, stepwise-MLR, and GFA-MLR were performed to achieve a reliable and robust model. The QSAR models obtained indicated the impact of molecular properties such as van der Waals surface area combination with the electrostatic property, the number of double bonds and rotatable bonds, partial charge, hydrophilic properties and molecular potential energy in the binding affinity, and selectivity of $A_{2A}R$ antagonist to Xanthine-type PET tracers. The provided model could be a helpful tool in the prediction of the $A_{2A}R$ binding affinity and $A_{2A}R$ selectivity, in a fast and costless manner, for any future studies that may require an estimation of these important characteristics of $A_{2A}R$ antagonist PET tracers.

Docking study reveals that the π - π stacking interactions between aromatic ligand and triazine core was the common interaction pattern in the binding affinity and selectivity of $A_{2A}R$ antagonist to Xanthine-type PET tracers. The importance of hydrogen bonding interactions of ligands and amino group of $A_{2A}R$ antagonist was also confirmed.

Compliance with ethical standards

Conflict of interest The authors declare that they have no conflict of interest.

References

- Müller CE, Scior T (1993) Adenosine receptors and their modulators. *Pharm Acta Helv* 68(2):77–111
- Sachdeva S, Gupta M (2013) Adenosine and its receptors as therapeutic targets: an overview. *Saudi Pharm J* 21(3):245–253
- Dunwiddie TV, Masino SA (2001) The role and regulation of adenosine in the central nervous system. *Annu Rev Neurosci* 24(1):31–55
- Fredholm BB, Abbracchio MP, Burnstock G, Daly JW, Harden TK, Jacobson KA, Leff P, Williams M (1994) Nomenclature and classification of purinoceptors. *Pharmacol Rev* 46(2):143–156
- Haas HL, Selbach O (2000) Functions of neuronal adenosine receptors. *Naunyn-Schmiedeberg's arch. Pharmacology* 362(4–5):375–381

6. Poulsen S-A, Quinn RJ (1998) Adenosine receptors: new opportunities for future drugs. *Bioorg Med Chem* 6(6):619–641
7. Kim DS, Palmiter RD (2003) Adenosine receptor blockade reverses hypophagia and enhances locomotor activity of dopamine-deficient mice. *Proc Natl Acad Sci* 100(3):1346–1351
8. Pinna A (2014) Adenosine A2A receptor antagonists in Parkinson's disease: progress in clinical trials from the newly approved istradefylline to drugs in early development and those already discontinued. *CNS Drugs* 28(5):455–474
9. Jacobson KA, Van Galen PJ, Williams M (1992) Adenosine receptors: pharmacology, structure-activity relationships, and therapeutic potential. *J Med Chem* 35(3):407–422
10. Cools AR, Rossum JV (1976) Excitation-mediating and inhibition-mediating dopamine-receptors: a new concept towards a better understanding of electrophysiological, biochemical, pharmacological, functional and clinical data. *Psychopharmacology* 45(3):243–254
11. Ongini E, Adami M, Ferri C, Bertorelli R (1997) Adenosine A2A receptors and neuroprotection. *Ann N Y Acad Sci* 825(1):30–48
12. Richardson PJ, Kase H, Jenner PG (1997) Adenosine A2A receptor antagonists as new agents for the treatment of Parkinson's disease. *Trends Pharmacol Sci* 18(4):338–344
13. Fenu S, Pinna A, Ongini E, Morelli M (1997) Adenosine a 2A receptor antagonism potentiates L-DOPA-induced turning behaviour and c-fos expression in 6-hydroxydopamine-lesioned rats. *Eur J Pharmacol* 321(2):143–147
14. Kanda T, Jackson MJ, Smith LA, Pearce RK, Nakamura J, Kase H, Kuwana Y, Jenner P (1998) Adenosine A2A antagonist: a novel antiparkinsonian agent that does not provoke dyskinesia in parkinsonian monkeys. *Ann Neurol* 43(4):507–513
15. Kanda T, Shiozaki S, Shimada J, Suzuki F, Nakamura J (1994) KF17837: a novel selective adenosine A2A receptor antagonist with anticataleptic activity. *Eur J Pharmacol* 256(3):263–268
16. Mally J, Stone TW (1996) Potential role of adenosine antagonist therapy in pathological tremor disorders. *Pharmacol Ther* 72(3):243–250
17. Shimada J, Koike N, Nonaka H, Shiozaki S, Yanagawa K, Kanda T, Kobayashi H, Ichimura M, Nakamura J, Kase H (1997) Adenosine A 2A antagonists with potent anti-cataleptic activity. *Med Chem Lett* 7(18):2349–2352
18. Shiozaki S, Ichikawa S, Nakamura J, Kitamura S, Yamada K, Kuwana Y (1999) Actions of adenosine A2A receptor antagonist KW-6002 on drug-induced catalepsy and hypokinesia caused by reserpine or MPTP. *Psychopharmacology* 147(1):90–95
19. Segovia F, Górriz J, Ramírez J, Salas-Gonzalez D, Álvarez I, López M, Chaves R, Initiative AsDN (2012) A comparative study of feature extraction methods for the diagnosis of Alzheimer's disease using the ADNI database. *Neurocomputing* 75(1):64–71
20. Zhang D, Wang Y, Zhou L, Yuan H, Shen D, Initiative AsDN (2011) Multimodal classification of Alzheimer's disease and mild cognitive impairment. *NeuroImage* 55(3):856–867
21. Alavi A, Basu S (2008) Planar and SPECT imaging in the era of PET and PET-CT: can it survive the test of time? *Eur J Nucl Med Mol Imaging* 35(8):1554–1559
22. Rahmim A, Zaidi H (2008) PET versus SPECT: strengths, limitations and challenges. *Nucl Med Commun* 29(3):193–207
23. Holschbach MH, Olsson RA (2002) Applications of adenosine receptor ligands in medical imaging by positron emission tomography. *Curr Pharm Des* 8(26):2345–2352
24. Elsinga PH, Hatano K, Ishiwata K (2006) PET tracers for imaging of the dopaminergic system. *Curr Med Chem* 13(18):2139–2153
25. Ishiwata K, Kimura Y, de Vries J, Erik F, Elsinga PH (2007) PET tracers for mapping adenosine receptors as probes for diagnosis of CNS disorders. *Cent Nerv Syst Agents Med Chem* 7(1):57–77
26. Ghasemi J, Salahinejad M, Rofouei M (2011) Review of the quantitative structure-activity relationship modelling methods on estimation of formation constants of macrocyclic compounds with different guest molecules. *Supramol Chem* 23(9):614–629
27. Salahinejad M, Ghasemi J (2014) 3D-QSAR studies on the toxicity of substituted benzenes to *Tetrahymena pyriformis*: CoMFA, CoMSIA and VolSurf approaches. *Ecotoxicol Environ Saf* 105:128–134
28. Du Q-S, Huang R-B, Chou K-C (2008) Recent advances in QSAR and their applications in predicting the activities of chemical molecules, peptides and proteins for drug design. *Curr Protein Pept Sci* 9(3):248–259
29. Khanapur S, van Waarde A, Ishiwata K, Leenders KL, Dierckx RA, Elsinga PH (2014) Adenosine A2A receptor antagonists as positron emission tomography (PET) tracers. *Curr Med Chem* 21(3):312–328
30. Guyon I, Elisseeff A (2003) An introduction to variable and feature selection. *J Mach Learn Res* 3:1157–1182
31. Holland JH (1992) Adaptation in natural and artificial systems: an introductory analysis with applications to biology, control, and artificial intelligence. MIT Press, Cambridge
32. Ayers JT, Clauset A, Schmitt JD, Dwojskin LP, Crooks PA (2005) Molecular modeling of mono- and bis-quaternary ammonium salts as ligands at the $\alpha 4\beta 2$ nicotinic acetylcholine receptor subtype using nonlinear techniques. *AAPS J* 7(3):E678–E685
33. Vadlamudi SM, Kulkarni VM (2003) 3D-QSAR of protein tyrosine phosphatase 1B inhibitors by genetic function approximation. *Internet Electron J Mol Des* 2:000
34. Mercader AG, Duchowicz PR, Fernández FM, Castro EA (2008) Modified and enhanced replacement method for the selection of molecular descriptors in QSAR and QSPR theories. *Chemom Intell Lab Syst* 92(2):138–144
35. Duchowicz PR, Castro EA, Fernández FM (2006) Alternative algorithm for the search of an optimal set of descriptors in QSAR-QSPR studies. *MATCH Commun Math Comput Chem* 55:179–192
36. Duchowicz PR, Fernández M, Caballero J, Castro EA, Fernández FM (2006) QSAR for non-nucleoside inhibitors of HIV-1 reverse transcriptase. *Bioorg Med Chem* 14(17):5876–5889
37. Rücker C, Rücker G, Meringer M (2007) Y-randomization and its variants in QSPR/QSAR. *J Chem Inf Model* 47(6):2345–2357
38. Roy K, Das RN, Ambure P, Aher RB (2016) Be aware of error measures. Further studies on validation of predictive QSAR models. *Chemom Intell Lab Syst* 152:18–33
39. Roy K, Kar S, Ambure P (2015) On a simple approach for determining applicability domain of QSAR models. *Chemom Intell Lab Syst* 145:22–29
40. Choi H, Lee DS (2015) PET and SPECT of neurobiological systems. *J Nucl Med* 56(11):1805–1805
41. Chirico N, Gramatica P (2011) Real external predictivity of QSAR models: how to evaluate it? Comparison of different validation criteria and proposal of using the concordance correlation coefficient. *J Chem Inf Model* 51(9):2320–2335
42. Stigliani J-L, Bernardes-Génisson V, Bernadou J, Pratiel G (2012) Cross-docking study on InhA inhibitors: a combination of Autodock Vina and PM6-DH2 simulations to retrieve bio-active conformations. *Org Biomol Chem* 10(31):6341–6349